

Resistivity of the liquid gallium-lead miscibility gap systemA. Ben Abdellah,^{1,2} J. G. Gasser,^{2,*} A. Makradi,^{2,3} B. Grosdidier,² and J. Hugel²¹*Electronics and Microwaves Group, UFR (Electronique et Physique du Solide), Faculty of Science, Abdelmalek Essaadi University, P.O. Box 2121, Tetuan 93000, Morocco*²*Laboratoire de Physique des Liquides et des Interfaces, Institut de Physique-électronique et Chimie, Université de Metz, 1 Boulevard Arago 57078, Metz Cedex 3, France*³*Center for Advanced Engineering Fibers and Film, School of Textiles, Fiber and Polymer Science, Clemson University, 161 Serrine Hall, Box 340971, Clemson, South Carolina 2963-0971, USA*

(Received 2 December 2002; revised manuscript received 23 July 2003; published 3 November 2003)

We present our electrical resistivity measurements of the gallium-lead system which shows a very large miscibility gap between 2.4 and 94.5 at. % lead with a critical temperature of 606 °C and composition of 40 at. % lead. A small negative deviation of the experimental temperature coefficient of the resistivity (TCR) appears near the critical composition of the alloy. The resistivity of the alloys is interpreted and discussed in terms of the extended Faber-Ziman formula using the t -matrix formalism with hard-sphere and experimental (for pure metals only) structure factors. An approach is proposed, taking into account the information given by the experimental density of states which allowed us to explain the resistivity of pure lead and that of the liquid gallium-lead alloys. As a conclusion it was shown that two electrons in the conduction band of liquid lead better explain the experimental resistivity than four electrons.

DOI: 10.1103/PhysRevB.68.184201

PACS number(s): 61.25.Mv

I. INTRODUCTION

Over the last decade the formation of chemical short-range order in liquid metallic alloys has been the subject of increasing attention. The understanding of the mixing behavior of two elemental metals forming a binary alloy has always attracted interest for physicists and metallurgists. The positive enthalpy of mixing can induce the miscibility gap of the liquid alloys. Several classical experimental methods: chemical analysis,¹⁻³ thermal analysis,⁴⁻⁶ neutron scattering on Li-Na,⁷ Cu-Pb,⁸ Bi-Zn,⁹ and more recently the isopiestic technique,¹⁰ have been used to measure the degree of immiscibility in phase-separating liquid alloys. It is interesting to investigate the effect of the immiscibility on the electronic transport properties of these alloys.

Most liquid alloys composed of nontransition metals behave as nearly free electron conductors, and their electronic properties can be well described by the theory of Faber and Ziman¹¹ which was originally developed by Ziman¹² for pure normal metals and was “extended” by Evans *et al.*¹³ to apply to liquid noble and transition metals. They simply replace the weak ion pseudopotential in the Ziman theory¹² by the t matrix determined using the muffin-tin approximation expressed in terms of phase shifts. Within the “extended Ziman formalism,” two approaches have been developed. The first one was initiated by Dreirach *et al.*¹⁴ and the second one by Esposito *et al.*¹⁵ The main difference lies in the fact that the former includes only **s** and **p** electrons to form the conduction band whereas the latter also takes into account the **d** electrons. The electronic transport properties of liquid metals are based on the scattering of nearly free electrons by potentials. We used an approach called the “method of the neutral pseudoatoms” introduced by Ziman.¹⁶ It starts with the muffin-tin potential of an atom and takes into account the exchange contribution through a Slater¹⁷ (or Kohn-Sham¹⁸) formula. This method was first used for liquid metals by

Dreirach¹⁹ and for liquid alloys by Dreirach *et al.*,¹⁴ Hirata *et al.*,²⁰ and other authors. We used a description of the exchange and correlation effects²¹ by employing either the local density approximation (LDA)²² approach only, or the LDA approach with a generalized gradient approximation (GGA) contribution.²³⁻²⁵ It is clear that the position of the Fermi energy, with respect to the scattering muffin-tin potential, plays an essential role in the electronic transport properties. Its position depends on the location of the conduction band bottom relative to the muffin-tin zero and on the shape of the density of states. Dreirach *et al.*¹⁴ assumed a free electron density of states band whose bottom is shifted by E_B from the muffin-tin zero [Fig. 1(a)]. The E_B value is calculated following an expression due to Ziman²⁶ and discussed explicitly by Ballentine *et al.*²⁷ Esposito *et al.*¹⁵ postulate that the bottom of the free electron band is located at the muffin-tin zero [Fig. 1(b)]. But they take into account the true shape of the conduction band by using Lloyd’s formula²⁸ to calculate the integrated density of states. In this work, we make a synthesis of the two approaches, and take into account the fact that, according to the experimental total density of states,²⁹ the liquid lead is split into two bands separated by a gap. The $6p$ band is located above the $6s$ states and is separated by a genuine energy gap.²⁹ We take into account this experimental information in order to describe the shape and the position of the p conduction band [Fig. 1(c)].

In Sec. II we recall the theoretical formula of the resistivity and the calculation of bottom of the free electron band. We describe the experimental method in Sec. III. Our experimental results are presented in Sec. IV and are discussed semiquantitatively.

II. THEORY

A still unsolved problem is the number of conduction electrons of liquid lead. Nearly all earlier papers consider

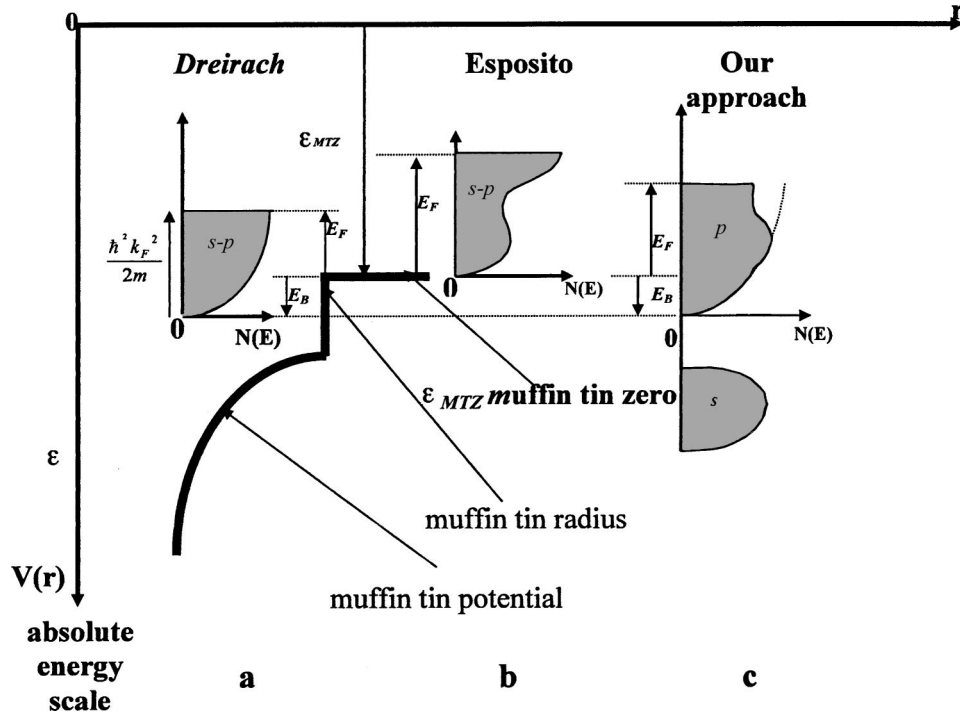


FIG. 1. Determination of the Fermi energy following the methods of Dreirach, Esposito, and our approach. The muffin-tin potential $V(r)$ is represented on an absolute scale of energy where ε is the energy necessary to put an electron at infinity with a velocity zero. We use a second reference of energy E . The zero corresponds to the muffin-tin zero potential. (a) Dreirach approach: the bottom of the conduction band is located at E_B from the muffin-tin zero; E_B can be positive or negative. The band is a free electron band including s and p electrons. (b) Esposito approach: the bottom of the conduction band is located at the muffin-tin zero ($E_B=0$); the band is a free electron band corrected by using the scattering theory expression of Esposito *et al.* (Ref. 15) derived originally by Lloyd (Ref. 28). It may include a d electron band. (c) Our approach: we separate the s - p band into a s and p band following experimental DOS (Ref. 29). The p band is shifted by E_B as Dreirach *et al.* (Ref. 14) and the DOS is corrected by Lloyd's expressions given in the EEG paper.

that four electrons are accommodated in the conduction band. This is in opposition with the experimental density of state measured by Indlekofer²⁹⁻³¹ and Wotherspoon³² where a valence of 2 seems more adequate. Similarly, theoretical density of states (DOS) calculations of solid lead within a semirelativistic augmented plane wave (APW) method by Zdetsis *et al.*³³ and of liquid lead by Jank and Hafner³⁴ lead to the same conclusions. So it is of interest to test the effect of the valence on the electronic transport properties and to compare the results to our measurements. Chaib *et al.*³⁵ interpreted the resistivity and thermopower of liquid copper-lead using the same assumption ($Z=2$) and the crude Slater exchange contribution in the construction of the muffin-tin potential.

A. Expression of the resistivity

We express the electrical resistivity of a normal metal as a function of both the energy E and the wave vector \mathbf{k} following a scheme described by Makradi *et al.*²¹ using the Ziman¹² formula. The resistivity ρ can be written as function of energy:

$$\rho(E) = \frac{3\pi m_e^2 \Omega_0}{4e^2 \hbar^3 k^6} \int_0^{2k} a(q) |t(q, E)|^2 q^3 dq, \quad (1)$$

where Ω_0 is the atomic volume, q is the transfer wave vector, $a(q)$ is the structure factor, $t(q, E)$ is the t matrix expressed in terms of energy dependent phase shifts^{14,36}

$$t(q, E) = -\frac{2\pi\hbar^3}{m\sqrt{2mE}\Omega_0} \sum_l (2l + 1) \sin \eta_l(E) \exp[i\eta_l(E)] P_l(\cos \theta), \quad (2)$$

where $P_l(\cos \theta)$ are the Legendre polynomials and θ is the angle between the incident and the scattered wave vector. The phase shifts $\eta_l(E)$ are calculated from muffin-tin potentials constructed following the method of Mukhopadhyay *et al.*³⁷ The same formalism has also been applied to transition metals taking explicitly into account the fact that electrons with spin up and electrons with spin down do not feel the same potential.³⁸ To compare with the experimental resistivity, the formula (1) has to be taken at the Fermi energy ($E=E_F$) and at the Fermi wave vector ($k=k_F$).

The wave vector is written

$$k = \left(3\pi^2 \frac{N_C(E)}{\Omega_0} \right)^{1/3}. \quad (3)$$

k and E are related by $E = \hbar^2 k^2 / 2m_e + E_B$ (E_B is the bottom of the free electron band and will be discussed in Sec. II C). In the case of alloys, the expression $a(q)|t(q, E_F)|^2$ is replaced by

$$\begin{aligned} & t_1^2(q, E_F)[c(1-c) + c^2 a_{11}(q)] \\ & + t_2^2(q, E_F)[c(1-c) + (1-c)^2 a_{22}(q)] \\ & + t_1(q, E_F)t_2^*(q, E_F)c(1-c)[a_{12}(q) - 1/2] \\ & + t_1^*(q, E_F)t_2(q, E_F)c(1-c)[a_{12}(q) - 1/2]. \end{aligned} \quad (4)$$

The Fermi wave vector is obtained by a linear interpolation of the number of conduction electrons of the pure metals

$$N_C^{\text{alloy}}(E) = cN_C^{\text{Ga}} + (1-c)N_C^{\text{Pb}}. \quad (5)$$

The atomic volume is a linear interpolation of the atomic volume of pure metals

$$\Omega_0^{\text{alloy}} = c\Omega_0^{\text{Ga}} + (1-c)\Omega_0^{\text{Pb}}. \quad (6)$$

c is the concentration of the first species (gallium) and $(1-c)$ is the concentration for the second species (lead). The phase shifts are taken at the Fermi energy of each metal band. The number of conduction electrons is that of the alloy as in Dreirach *et al.*¹⁴ Of course this “two band model” is an approximation since we have to use and fill the “alloy density of states” band by the conduction electrons.

B. Muffin-tin potentials

The construction of the liquid lead and gallium potentials is based on the superposition of neutral atomic charge. The phase-shifts entering in the expression of the electronic properties are calculated from a muffin-tin potential using the LDA-GGA approximation. In all our calculations we use the exchange and correlation effects of Perdew, Burke, and Ernzerhof (PBE).²⁵

1. Hartree Fock formalism

In the framework of the Hartree-Fock (HF) theory, the atomic one particle potential is given by

$$v_a(r) = -\frac{z}{r} + \int \frac{\rho(r-r')}{|r-r'|} dr' + v_{\text{ex}}(r), \quad (7)$$

where z is the atomic number. The first and second terms are the potentials due, respectively, to the Coulomb interaction with the nuclear charge and with the other electrons. The last term is the exchange and correlation potential. The exchange correlation contribution has been approximated by Slater¹⁴ who introduced a weighted average over occupied states:

$$v_{\text{ex}}(r) = -3 \left[\left(\frac{3}{8\pi} \right) \rho(r) \right]^{1/3}, \quad (8)$$

where $\rho(r)$ is the local density of the system in question. This expression has been used by Chaïb *et al.*³⁵

2. Density functional theory

The density functional method provides a framework for the calculation of the ground state of atomic one particle potential. While density functional theory (DFT)²⁵ is exact in principle, a practical implementation of the method requires the approximation of the exchange-correlation potential. The simplest and most widely approximation used to calculate the exchange-correlation potential is the local-density approximation,²² which is valid only for slowly varying densities. The LDA has been improved with the development of the generalized gradient approximation^{23,24} in which the exchange-correlation functional incorporates density gradient terms. All details of the construction of the liquid single site potential and the superposed muffin-tin potentials are given in the paper of Makradi *et al.*²¹

C. Fermi energy determination

Two approaches are widely used for the determination of the Fermi energy.

1. Dreirach *et al.* method

The first method has been proposed by Dreirach *et al.*¹⁴ and has also been used by Hirata *et al.*²⁰ In this method the Fermi energy E_F is related to the muffin-tin zero potential [Fig. 1(a)] and can be written as

$$E_F = E_B + \frac{\hbar^2 k_F^2}{2m^*}, \quad (9)$$

where E_B is the bottom of the band and k_F is the free electron Fermi wave number. E_B is a structure independent quantity that can be related to the s -phase shift of the muffin-tin potential.^{26,27} The parameter m^* is an effective mass that Dreirach *et al.*¹⁹ determined from the band structure in the crystalline state. The energy E_F is counted from the muffin-tin zero energy [Fig. 1(a)] and not from the bottom of the free electron band.

2. The bottom of the conduction band

Ziman²⁶ has proposed a method to calculate the energy of the bottom of the band depending on the properties of the s - p - d wave phase shifts produced by a muffin-tin potential. This procedure enables us to numerically calculate the following results: For the lead at $T=750^\circ\text{C}$, the bottom of electron band is $E_B = -0.24$ Ryd and for the gallium at $T=550^\circ\text{C}$, the bottom of electron band is $E_B = -0.35$ Ryd.

3. Esposito *et al.* method

The second approach was presented by Esposito *et al.*¹⁵ who proposed a consistent method to determine E_F without any value of E_B and m^* . They introduced the number of conduction electrons per atom N_C (effective valence) which is different than the valence Z . The Fermi energy E_F is obtained by filling the density of states curve by Z electrons. The Fermi wave vector k_F is obtained from E_F by

TABLE I. Fermi energy E_F , bottom of the band E_B , “effective number of conduction electrons” N_C , and calculated resistivity (ρ) with Dreirach *et al.* (Ref. 14), Esposito *et al.* (Ref. 15), and our approach.

Metal	Lead ($Z=2$) approach 1	Lead ($Z=4$) approach 2	Gallium ($Z=3$)
Dreirach approach	$E_B = -0.24$ Ryd	$E_B = -0.24$ Ryd	$E_B = -0.35$ Ryd
	$N_C = 2$	$N_C = 4$	$N_C = 3$
	$E_F = 0.1655$ Ryd $\rho = 435.74 \mu\Omega \text{ cm}$	$E_F = 0.4038$ Ryd $\rho = 52.48 \mu\Omega \text{ cm}$	$E_F = 0.389$ Ryd $\rho = 51.93 \mu\Omega \text{ cm}$
Esposito approach	$E_B = 0$ Ryd	$E_B = 0$ Ryd	$E_B = 0$ Ryd
	$N_C = 2.51$	$N_C = 4.60$	$N_C = 3.58$
	$E_F = 0.47$ Ryd $\rho = 68.80 \mu\Omega \text{ cm}$	$E_F = 0.71$ Ryd $\rho = 39.37 \mu\Omega \text{ cm}$	$E_F = 0.8311$ Ryd $\rho = 33.82 \mu\Omega \text{ cm}$
Our approach	$E_B = -0.24$ Ryd	$E_B = -0.24$ Ryd	$E_B = -0.35$ Ryd
	$N_C = 2.68$	$N_C = 4.51$	$N_C = 3.75$
	$E_F = 0.2534$ Ryd $\rho = 148.11 \mu\Omega \text{ cm}$	$E_F = 0.4575$ Ryd $\rho = 46.67 \mu\Omega \text{ cm}$	$E_F = 0.5069$ Ryd $\rho = 30.07 \mu\Omega \text{ cm}$

$$k_F = \frac{(2mE_F)^{1/2}}{\hbar}. \quad (10)$$

The effective valence N_C is obtained from k_F by

$$N_C = \frac{k_F^3 \Omega_0}{3\pi^2}. \quad (11)$$

The interpretation of this prescription is based on Lloyd’s²⁸ expression for the total integrated density of states per atom appropriate to a system of nonoverlapping muffin-tin potentials:

$$N(E) = N_0(E) + \frac{2}{\pi} \sum_l (2l+1) \eta_l(E) + N_m(E). \quad (12)$$

$N_0(E)$ is the free-electron integrated density of states proportional to $E^{3/2}$, $\eta_l(E)$ the energy dependent phase shift of the single-site scattering, and $N_m(E)$ the effect of multiple scattering. In order to obtain the Fermi energy together with other free-electron parameters, consistent with the Faber-Ziman formula,³⁹ only single-site scattering has to be taken into account. According to Lloyd,²⁸ this implies that E_F has to be determined using the total number of valence electrons per atom in the conduction band:

$$Z = N(E_F) \approx N_0(E_F) + \frac{2}{\pi} \sum_l (2l+1) \eta_l(E_F). \quad (13)$$

The location of the Fermi energy with respect to the muffin-tin potential is illustrated in Fig. 1(b). The multiple-scattering term $N_m(E_F)$ has been neglected. This point may be a weakness of the approach but its importance has not been checked for computational reasons.

4. Our method

The Fermi energy has been determined with respect to the muffin-tin zero potential taken as the origin of the energy scale [Fig. 1(c)]. It depends on the integrated density of states $N(E)$ which has been obtained following Lloyd’s

method.²⁸ We have introduced the number of conduction electrons per atom N_c (effective valence) which is different than the valence Z . The Fermi energy is obtained by filling the density of states curve by Z electrons per atom. Contrarily to the Esposito *et al.* approach,¹⁵ we chose $E_B \neq 0$. This means that in our scheme the density of states $N(E)$ is shifted and, as a counterpart, the free density of states can no longer be corrected by Lloyd’s formula for electron energies below the muffin-tin zero. As a result, only electrons with an energy higher than the muffin-tin zero, give rise to a Lloyd’s contribution in the density of states. Thus we can summarize our approach as follows:

$$\begin{cases} N(E) \approx N_0(E) & \text{for } E_B < E < 0, \\ N(E) \approx N_0(E) + \frac{2}{\pi} \sum_l (2l+1) \eta_l(E) & \text{for } E > 0 \end{cases} \quad (14)$$

the Fermi wave vector is obtained from $k_F = \sqrt{2m(E_F - E_B)}/\hbar$ and N_c is obtained from k_F by formula (11). It cannot be considered as evident that the number of conduction electrons is $Z=4$ for liquid lead if one observes the experimental and theoretical densities of states.^{29–34} Thus we did the calculations within two assumptions: the first one with a conduction band containing four electrons and the second one with two separated bands. The latter assumption implies a lower band completely filled with two electrons and an upper band considered as the conduction band partially filled with the remaining two electrons. The resolution of Eq. (10) gives rise to the results reported in Table I which will be compared to the results obtained by Dreirach *et al.*¹⁴ and Esposito *et al.*¹⁵

III. EXPERIMENTAL DESIGN

Resistivity measurements were performed by using the four-probe method⁴⁰ with a quartz cell fitted with tungsten electrodes (Fig. 2). The resistance of the sample is given by $R = \rho C$, where C is the geometrical “cell constant” C

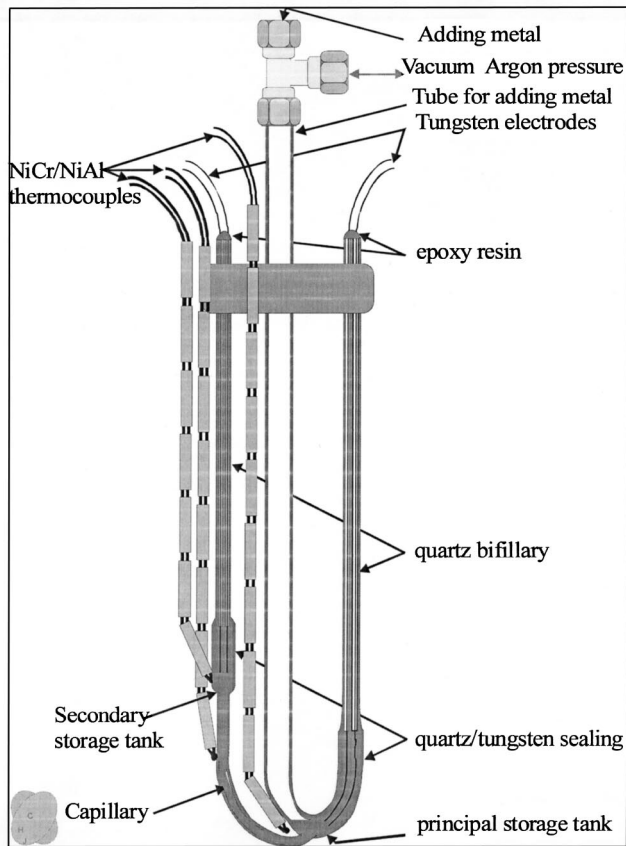


FIG. 2. Experimental measurement cell.

$= \int_0^l [dl/S(l)]$. The cell constant was determined at room temperature by using triple distilled mercury whose resistivity is well known. Since the variation of the cell constant due to the expansion from the room temperature up to 1100 °C is less than 0.5%, we have neglected this variation. The cell was used for the investigations of the entire concentration range of the phase diagram above the binodal curve (i.e., in the homogenous alloys). The measurements were made in 10 at. % steps. The temperature was measured with three chromel-alumel thermocouples in contact with the cell.

IV. RESULTS AND DISCUSSIONS

A. Experiments

The entire system was connected to vacuum or argon atmosphere. The alloys were prepared from gallium and lead supplied by Johnson and Matthey with a nominal purity of 99.999%. The experimental resistivity was measured with a resolution of better than 0.01% and an accuracy of 0.3%. To our knowledge, the electrical resistivity of gallium-lead alloy has only been measured by Kononenko *et al.*⁴¹ for the dilute alloys (until 1 at. % Pb) and by Sokolovskii *et al.*⁴² who have measured the “electroconductivity” of the same liquid alloy in the entire concentration-temperature range of the miscibility gap. Our resistivity measurements versus temperature for all compositions are presented in Fig. 3. The experimental data have been fitted by fourth-order polynomials namely $\rho = a_0 + a_1T_c + a_2T_c^2 + a_3T_c^3 + a_4T_c^4$ and the coefficients are re-

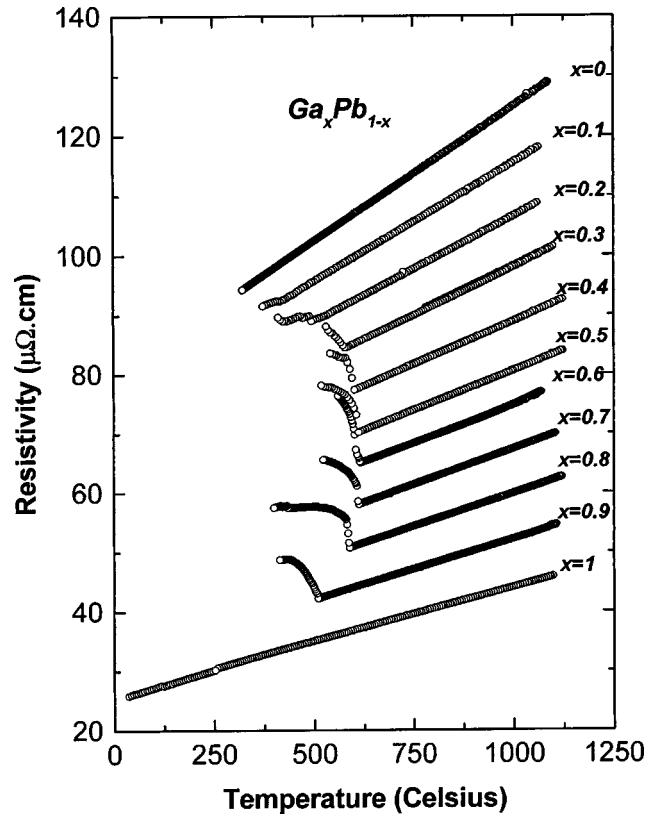


FIG. 3. Experimental electrical resistivity of liquid gallium-lead alloys as a function of temperature for different atomic concentrations.

ported in Table II. The difference between the polynomial and our experimental result is lower than 0.03% below 1000 °C.

When the temperature decreases, it appears clearly in Fig. 3 that, at a certain temperature, the resistivity increases rapidly. The observed phenomenon indicates that we reach the miscibility gap temperature. Thus the resistivity behavior reveals to be a useful tool to determine the binodal curve or more generally the liquidus curve.

We summarize in Table III the temperatures of the phase separation (T_s) that we obtain and we compare these values to those of the literature. We obtain a “critical temperature” of 616 °C. However, it is useful to precise that our alloy is not homogenous in temperature along the capillary. Thus the observed phenomenon occurs when the lowest temperature of the capillary reaches the miscibility gap. It introduces consequently an error of about 5 °C.

The obtained value of 616 °C is 10 °C higher than the literature value (Massalski)⁴³ and lower by about 12 °C than that of Sokolovskii *et al.*⁴² Concerning the resistivity, the difference between their values and ours is more than 20%. Since the temperature dependence of the resistivity is linear, this disagreement does not influence the resistivity but overestimates the liquidus curve. The remaining difference may be attributed to the uncertainty in temperature measurements or to the prescriptions used for measuring the diagram reported in Massalski.⁴³ We can observe that all the resistivities seem to be a linear function versus temperature both for pure

TABLE II. Coefficients of polynomials fitted on the experimental resistivity of liquid $\text{Ga}_x\text{Pb}_{1-x}$ alloys at different gallium concentration x_{Ga} .

x_{Ga}	a_0 ($\mu\Omega \text{ cm}$)	$a_1 \times 10^2$ ($\mu\Omega \text{ cm C}^{-1}$)	$a_2 \times 10^5$ ($\mu\Omega \text{ cm C}^{-2}$)	$a_3 \times 10^8$ ($\mu\Omega \text{ cm C}^{-3}$)	$a_4 \times 10^{12}$ ($\mu\Omega \text{ cm C}^{-4}$)	Between T ($^\circ\text{C}$)
1	25.057	2.0660	0.1486	-0.7478	4.3039	30-1100
0.9	35.237	-0.0324	4.6126	-4.4424	15.5512	509-1100
0.8	38.956	1.3250	2.1823	-2.2407	8.2353	589-1100
0.7	41.552	2.9000	-0.1655	-0.4923	3.4012	612-1100
0.6	61.787	4.4430	14.9321	-14.2702	50.8363	616-1100
0.5	44.481	7.0560	-7.4336	5.4135	-14.2730	612-1100
0.4	50.159	7.4250	-7.6648	5.5713	-14.5684	601-1100
0.3	67.746	1.9790	2.9519	-3.0976	11.8924	577-1100
0.2	73.498	2.0220	3.61410	-3.73122	13.3985	526-1100
0.1	73.278	5.0580	-1.4744	0.60707	0.28780	415-1100
0	78.703	5.0460	-0.7350	-0.1846	1.2015	327-1100

metals and for liquid alloys above the phase separation temperature T_s . The nonlinearity which appears in Table I is small if one observes Fig. 3. The experimental resistivity temperatures coefficients of the liquid $\text{Ga}_x\text{-Pb}_{(1-x)}$ alloys versus the temperature ($T=630, 700,$ and 800°C) and concentration are presented in Fig. 4. The TCR coefficient decreases linearly with the gallium concentration. A relative minimum of the TCR appears at the critical composition when the critical temperature is approached. We interpret the phenomenon by relating it to the divergence of the structure factor at long wavelength limits (small q values). The divergence of the structure factor at low angles has been observed for other liquid alloys [Cu-Pb (Ref. 8) and Bi-Zn (Refs. 44, 45)] which also present a miscibility gap.

By analyzing the experimental measurements devoted to the electrical properties of segregated and demixed liquid alloys, we note that Schürman and Parks⁴⁶ measured the resistivity of the demixing alloy (Ga-Hg) but that they observed no anomaly in the derivative of the resistivity. However, they showed a strong divergence of the specific heat.⁴⁷ Schürman and Parks⁴⁸ also observed that for the liquid

TABLE III. Temperatures of phase separation (T_s) with the corresponding resistivities compared to the literature values.

x_{Ga}	This work		Sokolvskii <i>et al.</i> (Ref. 42)		Massalski (Ref. 43)
	T_s (C)	ρ_{exp} ($\mu\Omega \text{ cm C}$)	T_s (C)	ρ_{exp} ($\mu\Omega \text{ cm C}$)	T_s (C)
0.9	509	42.22			517
0.8	589	50.66	565	42.6	583
0.7	609	58.53	603	45.0	602
0.6	616	65.02	628	51.1	606
0.5	612	70.18			604
0.4	601	77.35	628	59.4	595
0.3	577	84.50			576
0.2	526	88.97	596	68.8	536
0.1	415	92.35			442

sodium-lithium alloy, the TCR presents a positive peak at the critical composition and at the critical temperature. Philippov *et al.*⁴⁹ have observed a large negative deviation of the temperature coefficient of the sound velocity near the critical composition for Ga-Pb. They indicated a similar behavior of the temperature coefficient of the adiabatic compressibility. It is known that the adiabatic compressibility is related to the structure factor at the long wavelength limit [$S(0)$] which exhibits a divergence for this kind of alloy.

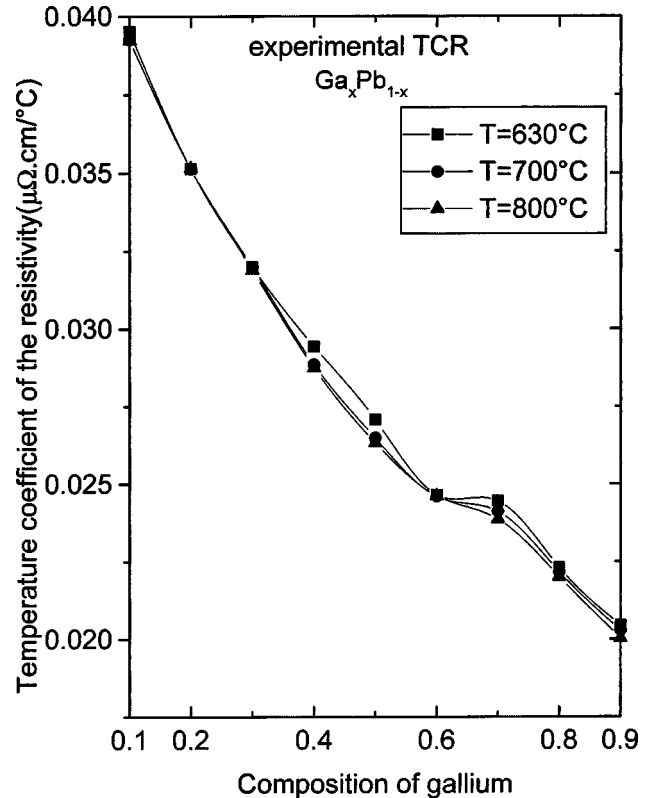


FIG. 4. Isotherm of the temperature coefficient of the resistivity of gallium-lead at $T=630, 700,$ and 800°C near the miscibility gap.

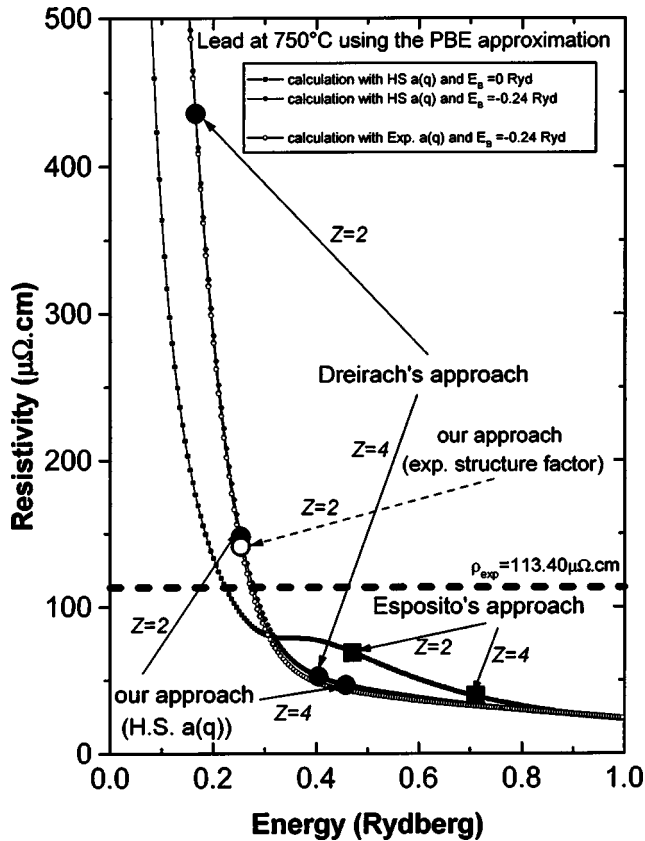


FIG. 5. Energy dependence of the electrical resistivity of liquid lead compared to our measurement.

B. Theoretical investigation discussion

For the theoretical interpretation of our experimental results, we used the extended formula of Faber and Ziman expressed in terms of the phase shifts. We have calculated the phase shifts as a function of the energy for electrons scattered by a muffin-tin potential. Its construction has been adapted to the liquid metals by Hugel *et al.*⁵⁰ and supplemented by the recent contribution of PBE's exchange-correlation potential.²⁵

Based on the Indlekofer experimental determination of the density of state derived from UPS spectra²⁹⁻³² we have assumed that the outer $6s^2$ and $6p^2$ electrons are split into two individual bands. This means that the lower band filled to the top with two electrons cannot be considered as participating to the conduction process. The remaining two electrons occupy the energy states of an unfilled conduction band which serves in our approach for the determination of the Fermi level.

1. Resistivity as function of energy for pure metals

Lead. We calculate the resistivity as a function of energy by using the muffin-tin potentials constructed as described in Sec. II B. Two curves are plotted in Fig. 5, the first one corresponding to $E_B = 0$ (Esposito approach) and the second one to $E_B = -0.24$ Ryd (Dreirach and our approach). Both curves use the hard sphere structure factor with a packing fraction obtained with Waseda's formula 3.1.1 of Ref. 51

[$\eta(T) = A \exp(-BT)$]. It appears that if one uses Dreirach's approach (free electron density of states and $E_B \neq 0$) the resistivity obtained with four conduction electrons ($52.48 \mu\Omega \text{ cm}$: Table I) underestimates the experimental resistivity ($113.4 \mu\Omega \text{ cm}$). On the other hand a valence of $Z = 2$ overestimates it ($435.7 \mu\Omega \text{ cm}$). With the approach of Esposito ($E_B = 0$ and density of states determined with Lloyd's formula) we obtain 39.4 and $68.8 \mu\Omega \text{ cm}$ with, respectively, $Z = 4$ and $Z = 2$. We are far from the experimental value. But there is no reason that the bottom of the band starts from the muffin-tin zero energy. Furthermore, there is no reason that the band is free-electron-like as has been shown by an experimental determination of the density of states.²⁹⁻³¹ Thus the only reasonable approach seems us to be a combination of Esposito and Dreirach approaches taking into account the informations given by UPS spectra.²⁹⁻³¹ In our approach we obtain, with $Z = 4$, $46.67 \mu\Omega \text{ cm}$ which is two and a half times smaller than the experimental resistivity. If we use the value $Z = 2$ we obtain $148.11 \mu\Omega \text{ cm}$ which is 30% above the experimental resistivity. The agreement with the experimental resistivity can be improved by a few percent if, instead of using the hard sphere structure factor, we use the experimental structure factor. We obtain $141.34 \mu\Omega \text{ cm}$ which is now 24.6% above the experimental value. It appears that within the model used for the DOS and the resistivity calculation a valence 4 for lead does not give the best agreement with experiment.

Other experimental and theoretical values also conclude in the same way. The calculation of Jank and Hafner³⁴ show "a $6s$ band which is separated from the $6p$ band by a gap of $1-2$ eV related to relativistic effects, which tend to lower the s states relative to the higher-angular-momentum states." Hüttner⁵² measured the optical properties of lead and concluded that lead is far from showing Drude's behavior. He attributed it to interband effects confirming earlier measurements of Inagaki *et al.*⁵³ No definite conclusions can be obtained from Hall effect measurements.^{54,55} The experimental situation is not clear since the valence obtained in a free electron model goes from 1.5 to 3.5 electrons per atom. However, a free electron model cannot be used to interpret measurements as emphasized by Ballentine⁵⁶ who introduced a contribution due to "skew scattering."

Gallium. The resistivity of liquid gallium has been studied by Ben Hassine *et al.*⁵⁷ using Slater and Kohn Sham exchange and correlation. Presently, using the LDA-GGA expression one can observe in Fig. 6 that our results are improved. The density of states of Indlekofer⁵⁸ indicates that the DOS is near that of a free electron one. It is clear that we have to take $Z = 3$. In Fig. 6 we represent the resistivity calculated with $E_B = 0$ (Esposito approach) and $E_B = -0.35$ Ryd (Dreirach *et al.*¹⁴ and our approach). Our approach takes into account the deviation from the free electron DOS given by Lloyd in the determination of E_F .

We also represent the curve calculated with the experimental structure factor (at $E_B = -0.35$ Ryd only). It appears that this curve differs only at higher energies than the Fermi energy. Taking the hard sphere structure factor does not alter the resistivity.

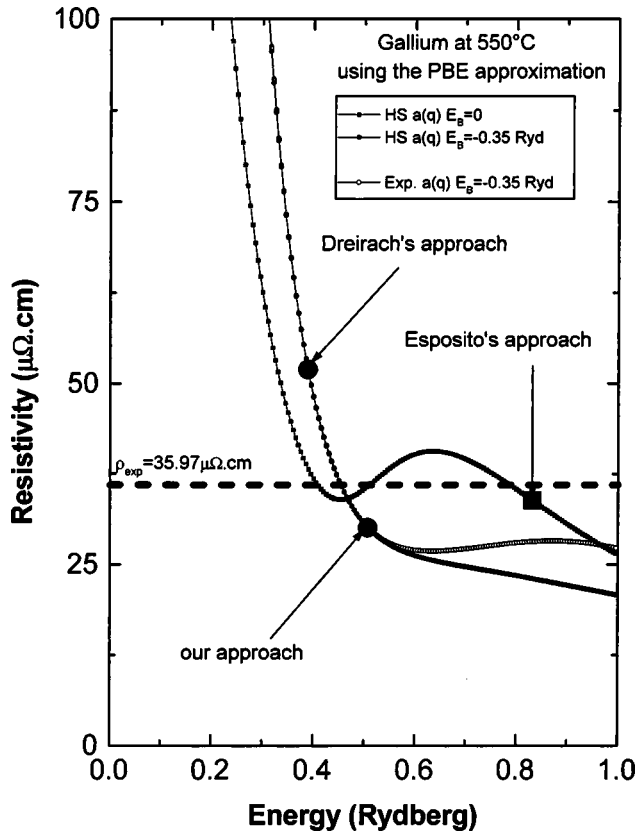


FIG. 6. Energy dependence of the electrical resistivity of liquid gallium compared to our measurement (horizontal line).

2. Resistivity of alloys

We represent the resistivity as a function of concentration in Fig. 7. It appears clearly that with $Z=4$ for liquid lead, the resistivity of the alloy is systematically underestimated. The only calculation which gives an acceptable result is our approach which is a compromise of Dreirach's and Esposito's concepts with $Z=2$. The remaining "discrepancy" can be attributed to the inherent inaccuracy of such a calculation. Indeed a small error in the experimental pair correlation function used to construct the muffin-tin potential can have an important effect on the resistivity. We have also fitted the calculated resistivity on the experimental one for pure metals. We obtain a Fermi energy of lead of $E_F=0.2878$ Ryd, which corresponds to $N_c=2.97$ and a Fermi energy of pure gallium of $E_F=0.4322$ Ryd, which corresponds to $N_c=3.34$. The calculated resistivity of the alloy is very near the experimental curve. We can conclude that the structure of the alloy is pretty well described with our calculated HS structure factor. The main contribution to the resistivity comes from the first peaks of the structure factors. Its divergence at low q values has only a small effect on the temperature coefficient.

However, a weakness of our calculation may stem from the fact that we combine the density of states of pure lead and gallium. In fact we can consider that the true alloy density of state is the result of a mixing of the two individual densities. This means that, on alloying, the band gap between

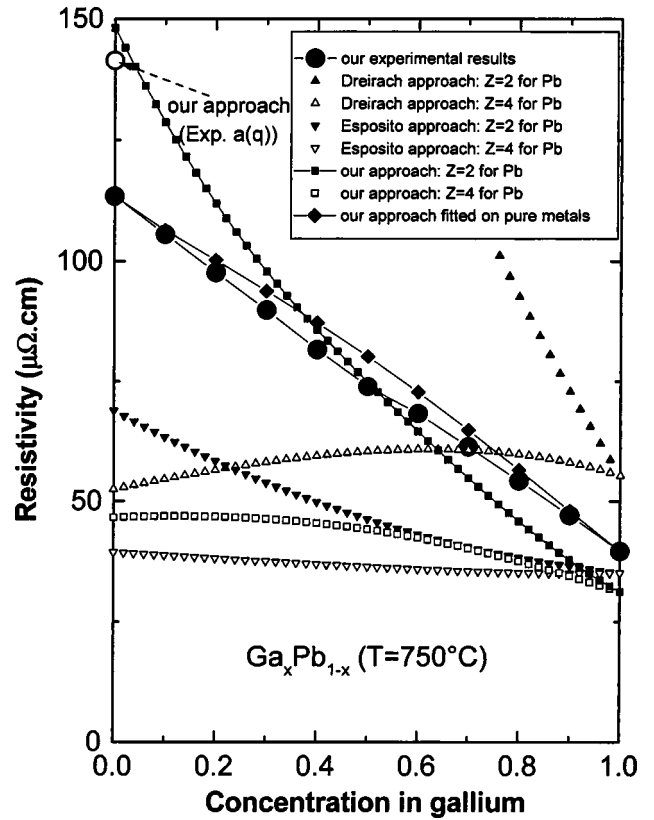


FIG. 7. Comparison between experimental and calculated resistivities of liquid lead-gallium alloys as a function of atomic concentration at 750 °C. We plot six *ab initio* calculations with $Z=2$ and $Z=4$ using Dreirach, Esposito, and our approach. We also compare our experiment to a calculation where the Fermi energy is fitted in order to obtain the experimental resistivity for the pure metals.

$6s$ and $6p$ bands is progressively filled. But as the partial resistivities are weighted by the square of the concentration, the lead rich alloys behave as if the the valency of lead is 2, while on the gallium rich side we may take a valency of 4, the square of the concentration minimizes this contribution.

V. CONCLUSION

In conclusion, our approach, inspired by the experimental density of states, allows a satisfactory explanation of the resistivity of lead and gallium as well as that of the liquid gallium-lead alloys. The results presented in Fig. 7 clearly show that the resistivity calculated from a conduction band occupied with two electrons is revealed to be closer to experiment. The raised question of whether the conduction band of liquid lead contains two or four electrons appears to us definitively in favor of a conduction band occupied by two electrons in agreement with DOS, optical measurements, and calculations. The resistivity measurements are a very simple and efficient tool for the experimental determination of the liquidus. We have shown the existence of a small TCR anomalous behavior in the neighborhood of the critical point

of the liquid gallium lead alloy which may be related to the miscibility gap. It may be interesting to study the consequence of the electronic configuration on other physicals properties (structure factor, for example) using pseudopotential and molecular dynamic calculations.

ACKNOWLEDGMENTS

One of us (A.M.) thanks Professor Perdew for sending his subroutine of LDA-GGA contribution. The authors would like to acknowledge J.C. Humbert for technical assistance during the experiments.

*Corresponding author. Email address: gasser@sciences.univ-metz.fr

- ¹W. Claus and I. Hermann, *Metallwiss.* **18**, 957 (1939).
- ²L. W. Kempf and K. R. Van Horn, *Trans. AIME* **133**, 81 (1939).
- ³Y. Dardel, *Light Metals* **9**, 220 (1946).
- ⁴T. Heumann and B. Predel, *Z. Metallkd.* **49**, 90 (1958).
- ⁵A. N. Campbell and R. W. Ashley, *Can. J. Res. Sect. B* **18**, 281 (1940).
- ⁶B. Predel and H. Sandig, *Mater. Sci. Rep.* **4**, 49 (1969).
- ⁷H. Ruppertsberg, *Z. Naturforsch. A* **32**, 1374 (1977).
- ⁸M. Favre Bonte, J. Bletry, P. Hicter, and P. J. Desre, *J. Phys. (Paris), Colloq.* **41**, 156 (1980).
- ⁹G. D. Wignall and P. A. Egelstaff, *J. Phys. C* **1**, 519 (1986).
- ¹⁰S. K. Yu, F. Sommer, and B. Predel, *Z. Metallkd.* **87**, 574 (1996).
- ¹¹T. E. Faber and J. M. Ziman, *Philos. Mag.* **11**, 153 (1965).
- ¹²J. M. Ziman, *Philos. Mag.* **6**, 1013 (1961).
- ¹³R. Evans, D. A. Greenwood, and P. Lloyd, *Phys. Lett.* **35A**, 57 (1971).
- ¹⁴O. Dreirach, R. Evans, H. Güntherodt, and U. Künzi, *J. Phys. F: Met. Phys.* **2**, 709 (1972).
- ¹⁵E. Esposito, H. Ehrenreich, and C. D. Gelatt, *Phys. Rev. B* **18**, 3913 (1978).
- ¹⁶J. M. Ziman, *Adv. Phys.* **13**, 89 (1964).
- ¹⁷J. C. Slater, *Phys. Rev.* **81**, 385 (1951).
- ¹⁸W. Kohn and L. Sham, *Phys. Rev. A* **10**, 1133 (1965).
- ¹⁹O. Dreirach, *J. Phys. F: Met. Phys.* **1**, L40 (1971).
- ²⁰K. Hirata, Y. Waseda, A. Jain, and R. Srivastava, *J. Phys. F: Met. Phys.* **7**, 419 (1977).
- ²¹A. Makradi, J. G. Gasser, J. Hugel, A. Yazı, and M. Bestandji, *J. Phys.: Condens. Matter* **11**, 671 (1999).
- ²²U. Von Barth and L. Hedin, *J. Phys. C* **5**, 1629 (1972).
- ²³J. P. Perdew and Y. Wang, *Phys. Rev. B* **33**, 8800 (1986).
- ²⁴J. P. Perdew, *Phys. Rev. B* **33**, 8822 (1986).
- ²⁵J. P. Perdew, K. Burke, and M. Ernzerhof, *Phys. Rev. Lett.* **77**, 3865 (1996).
- ²⁶J. M. Ziman, *Proc. Phys. Soc. London* **91**, 723 (1967).
- ²⁷L. E. Ballentine and M. Huberman, *J. Phys. C* **10**, 4991 (1977).
- ²⁸P. Lloyd, *Proc. Phys. Soc. London* **90**, 207 (1967).
- ²⁹G. Indlekofer, Ph.D. thesis, University Basel, Basel, 1987.
- ³⁰G. Indlekofer, A. Pflugı, and P. Oelhafen, *J. Non-Cryst. Solids* **117–118**, 351 (1990).
- ³¹P. Oelhafen, G. Indlekofer, and H. J. Güntherodt, *Z. Phys. Chem., Neue Folge* **157**, 483 (1988).
- ³²J. T. M. Wotherspoon, D. C. Rodway, and C. Norris, *Philos. Mag. B* **40**, 51 (1979).
- ³³A. D. Zdetis, D. A. Papacontantopoulos, and E. N. Economou, *J. Phys. F: Met. Phys.* **10**, 149 (1980).
- ³⁴W. Jank and J. Hafner, *Phys. Rev. B* **41**, 1497 (1990).
- ³⁵C. Chaı̈b, J. G. Gasser, J. Hugel, and L. Roubi, *Physica B* **252**, 106 (1998).
- ³⁶B. Delley and H. Beck, *J. Phys. F: Met. Phys.* **9**, 517 (1979).
- ³⁷G. Mukhopadhyay, A. Jain, and V. K. Ratti, *Solid State Commun.* **13**, 1623 (1973).
- ³⁸H. Zrouri, J. Hugel, A. Makradi, and J. G. Gasser, *Phys. Rev. B* **64**, 094202 (2001).
- ³⁹T. E. Faber and J. M. Ziman, *Philos. Mag.* **11**, 153 (1965).
- ⁴⁰J. Vinckel, N. Benazzi, H. Halim, J. G. Gasser, J. Comera, and P. Contamin, *J. Non-Cryst. Solids* **493**, 156 (1993).
- ⁴¹V. I. Kononenko and S. P. Yatsenko, *Dokl. Akad. Nauk SSSR* **18**, 70 (1968).
- ⁴²B. Sokolovskii, Yu. Plevachuk, and V. Didoukh, *Phys. Status Solidi A* **148**, 123 (1995).
- ⁴³T. B. Massalski, H. Okamoto, P. R. Subramanian, and L. Kacprzak, *Binary Alloy Phase Diagrams* (ASM, Metals Park, OH, 1990).
- ⁴⁴Z. C. Wang, S. K. Yu, and F. Sommer, *J. Chem. Phys.* **90**, 379 (1993).
- ⁴⁵S. Karlhuber, A. Mikula, R. N. Singh, and F. Sommer, *J. Alloys Compd.* **283**, 198 (1999).
- ⁴⁶H. K. Schürman and R. D. Parks, *Phys. Rev. Lett.* **26**, 367 (1971).
- ⁴⁷H. K. Schürman and R. D. Parks, *Phys. Rev. B* **6**, 348 (1972).
- ⁴⁸H. K. Schürman and R. D. Parks, *Phys. Rev. Lett.* **27**, 1790 (1971).
- ⁴⁹V. V. Philippov and P. S. Popel, *J. Chim. Phys. Phys.-Chim. Biol.* **94**, 1158 (1997).
- ⁵⁰J. Hugel and J. G. Gasser, *J. Non-Cryst. Solids* **117**, 118 (1990).
- ⁵¹Y. Waseda, *The Structure Of Non-Crystalline Materials, Liquid and Amorphous Solids* (McGraw-Hill, New York, 1980).
- ⁵²B. Hüttner, *J. Phys.: Condens. Matter* **7**, 907 (1990).
- ⁵³T. Inagaki, E. T. Arakawa, A. R. Cathers, and K. A. Glastad, *Phys. Rev. B* **25**, 6130 (1982).
- ⁵⁴N. E. Cusack, *Rep. Prog. Phys.* **36**, 361 (1963).
- ⁵⁵G. Busch and H. J. Güntherodt, *Solid State Phys.* **29**, 235 (1974).
- ⁵⁶L. E. Ballentine, *Inst. Phys. Conf. Ser.* **30**, 188 (1977).
- ⁵⁷L. Ben Hassine, J. Auchet, and J. G. Gasser, *Philos. Mag. B* **82**, 1225 (2002).
- ⁵⁸G. Indlekofer, P. Oelhafen, R. Lapka, and H. J. Güntherodt, *Z. Phys. Chem., Neue Folge* **157**, 465 (1988).